Deepest mantle viscosity: Constraints from Earth rotation anomalies

W. R. Peltier[1] and R. Drummond[1]

Received 12 March 2010; revised 10 May 2010; accepted 18 May 2010; published 23 June 2010.

[1] The radial variation of viscosity from Earth's surface to the core-mantle boundary is most accurately determined on the basis of observations related to the glacial isostatic adjustment (GIA) process. Beneath a depth of approximately 1250 km the primary constraints available pertain to the anomalies in Earth's rotational state that have previously been shown to be intimately linked to the same GIA process responsible for postglacial sea level variability. It is demonstrated that these anomalies are capable of resolving a difference between D″ viscosity and that of the overlying region which extends upwards to the 1250 km depth horizon. A "trade-off" is shown to exist between the viscosities in these deepest mantle layers that may be resolved by the observed direction of true polar wander. **Citation:** Peltier, W. R., and R. Drummond (2010), Deepest mantle viscosity: Constraints from Earth rotation anomalies, *Geophys. Res. Lett.*, *37*, L12304, doi:10.1029/2010GL043219.

1. Introduction

[2] A recent re-focusing of global geodynamics research has occurred as a consequence of significant breakthroughs in mineral physics research. For example the discovery by *Murakami et al.* [2004] of a new phase transformation from Perovskite to a higher pressure post-Perovskite phase appears to have finally provided a beguilingly parsimonious explanation of the existence of the D″ layer that lies above the core-mantle boundary and has a thickness of 150–300 km. Although early work on the mantle convection process often interpreted this layer to be a simple thermal boundary layer [e.g., see *Yuen and Peltier*, 1980] this picture, which would suggest D″ to be a layer of very low viscosity, is no longer tenable (see *Peltier* [2007b] for a recent review of the history of D″ interpretations).

[3] A similarly important discovery of high pressure mineral physics has been the recognition of the existence of a "spin-transition" of iron that onsets in Magnesiowustite below a depth of approximately 1250 km [e.g., *Lin et al.*, 2005]. This is accompanied by significant changes in physical properties such as bulk modulus and bulk sound speed and is expected to occur continuously over a significant range of depth [*Persson et al.*, 2006]. Although there is as yet no direct measurement of the creep resistance associated with the spin transition of Fe^{2+} in ferropericlase, $(Mg_{1-x}Fe_xO)$, nor for the higher pressure post-Perovskite phase, the issue as to what the effective viscosity might be in these regions is clearly of considerable interest from the perspective of the global geodynamics. The goal in this paper is to address this important question.

2. Model Viscosity Parameterizations

[4] The work will be based upon consideration of the family of viscosity profiles illustrated on Figure 1. Figure 1 displays viscosity models of three different types and origins. The model labeled VM2 was that inferred by *Peltier* [1994, 1996] on the basis of a formal Bayesian inversion of the totality of data related to the GIA process, as reviewed by *Peltier* [1998, 2007a]. The VM5a model [*Peltier and Drummond*, 2008] is an approximation to VM2 consisting of a 5-layer fit in which each layer is assumed to have a constant viscosity. The only significant difference between VM2 and VM5a concerns the near surface structure. In VM2 the "lithosphere" is assumed to have a thickness of 90 km and to be perfectly elastic. In VM5a the lithosphere is taken to consist of a 60 km thick perfectly elastic upper layer beneath which lies a 40 km thick layer in which the viscosity equals 10^{22} Pa s. The shallow structure in VM5a was shown to enable the model to eliminate a significant misfit between predicted and geodetically observed horizontal motions over the North American continent. Superimposed upon the viscosity structures for these two models is the set of models labeled D″ which are to be the focus herein. The choice of the depth beneath which the viscosity in the D″ models is allowed to deviate from that in VM5a , namely ~1250 km, is based upon the fact that the variation of viscosity at shallower depth is "pinned" by the totality of the relative sea level data employed in the original Bayesian inverse. Below this depth the only constraint on viscosity is provided by Earth rotation anomalies, namely the speed and direction of true polar wander and the non-tidal acceleration of rotation (J2-dot [see *Peltier* [2007a]). This depth is also the approximate depth of onset of the spin transition in iron. The deeper boundary approximately 300 km above the cmb is taken to define the upper boundary of the D″ layer at which the phase transformation from Perovskite to post-Perovskite occurs.

3. Theoretical Methods

[5] The theoretical structure of the GIA model to be employed is embodied in an integral equation of Fredholm type that is referred to as the "Sea Level Equation" [*Peltier*, 1974, 1976; *Peltier and Andrews*, 1976; *Farrell and Clark*, 1976; *Clark et al.*, 1978; *Peltier et al.*, 1978]. Its solution provides a prediction of the time dependent separation of the surface of the ocean and the surface of the solid Earth, $S(\theta, \lambda, t)$ say, given only an input radial visco-elastic structure of the planetary interior and an input history of land ice thickness. The former includes a seismically

[1]Department of Physics, University of Toronto, Toronto, Ontario, Canada.

0094-8276/10/2010GL043219

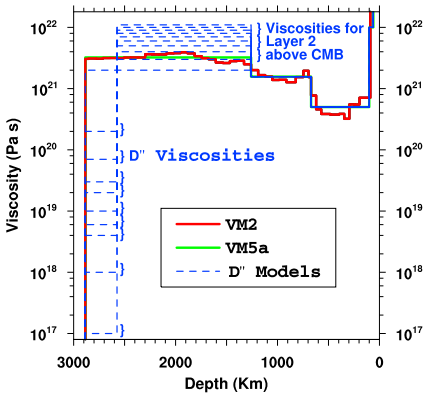

Figure 1. The family of mantle viscosity models discussed in this paper is that labeled D″. Also shown for comparison are models VM2 and VM5a. Model VM2 is that originally deduced by *Peltier* [1996] on the basis of a full Bayesian inversion of a large collection of data pertaining to the GIA process. Model VM5a is that produced by *Peltier and Drummond* [2008]. Beneath the surface lithosphere this model is a best fit multi-layer approximation to VM2. The lithosphere itself, however, rather than being described as a single perfectly elastic unit which is 90 km thick as in VM2, is stratified and consists of two distinct units. The upper unit is 60 km thick and is assumed to be perfectly elastic. The lower unit is 40 km thick and is assumed to be characterized by a viscosity of 10^{22} Pa s.

derived model of elastic wave velocities and density, e.g., the PREM model of *Dziewonski and Anderson* [1981], as well as a radial variation of effectively Newtonian viscosity which is the focus of this paper. The latter consists of an ice thickness history $I(\theta, \lambda, t)$ which contributes to a total surface mass load history $L(\theta, \lambda, t)$ which may be assumed to have the composite form:

$$L(\theta,\lambda,t) = \rho_I I(\theta,\lambda,t) + \rho_W S(\theta,\lambda,t), \tag{1}$$

in which ρ_I and ρ_W are the densities of ice and water respectively. In terms of these fields, the Sea Level Equation is:

$$\mathrm{S}(\theta,\lambda,\mathrm{t}) = \mathrm{C}(\theta,\lambda,\mathrm{t})\left[\int_{-\infty}^{\mathrm{t}} \mathrm{dt}' \iint_{\Omega} \mathrm{d}\Omega' \left\{ \mathrm{L}(\theta',\lambda',\mathrm{t}')\ \mathrm{G}_{\phi}^{\mathrm{L}}(\varphi,\mathrm{t}-\mathrm{t}') + \Psi^{R}(\theta',\lambda',t') G_{\phi}^{T}(\varphi,t-t') \right\} + \frac{\Delta\Phi(t)}{g}\right]. \tag{2}$$

[6] In (2) the function C is the so-called "ocean function" which is unity over the oceans and zero over the continents. The Green functions $G_{\phi}^{L}(\varphi, t)$ and $G_{\phi}^{T}(\varphi, t)$ are those which, when convolved with the surface mass load and tidal potential load, respectively, translate these respective loads into a impact upon the gravitational potential field at Earth' surface, an equipotential surface of which defines the surface of the equilibrium ocean. The field Ψ^{R} .is the space and time dependent variation in the centrifugal potential associated with the GIA process itself whereas $\Delta\Phi(t)/g$.is a time dependent but space independent correction required to ensure that the dynamical system conserves mass. Following *Dahlen* [1976] the space and time dependent expression for the GIA driven variation in the centrifugal potential, may be written, accurate to first order in perturbation theory, as:

$$\Psi^{\mathrm{R}}(\theta,\ \lambda,\ \mathrm{t}) = \Psi_{00}\, \mathrm{Y}_{00}(\theta,\ \lambda,\ \mathrm{t}) + \sum_{\mathrm{m}=-1}^{+1} \Psi_{2\mathrm{m}}\, \mathrm{Y}_{2\mathrm{m}}(\theta,\ \lambda,\ \mathrm{t}) \tag{3}$$

with

$$\Psi_{00} = \frac{2}{3}\, \omega_3\ (\mathrm{t})\ \Omega_{\mathrm{o}}\ \mathrm{a}^2 \tag{4a}$$

$$\Psi_{20} = -\frac{1}{3}\, \omega_3\ (\mathrm{t})\ \Omega_{\mathrm{o}}\ \mathrm{a}^2\ \sqrt{4/15} \tag{4b}$$

$$\Psi_{2,-1} = (\omega_1^{(\mathrm{t})} - \mathrm{i}\,\omega_2^{(\mathrm{t})})\ (\Omega_{\mathrm{o}}\ \mathrm{a}^2/2)\ \sqrt{2/15} \tag{4c}$$

$$\Psi_{2,+1} = -(\omega_1^{(t)} + i\omega_2(t))\ (\Omega_o\ a^2/2)\ \sqrt{2/15} \tag{4d}$$

[7] The ω_i in (4) are the variations in the Cartesian components of the Earth's angular velocity vector induced by the GIA process. In order to solve (2) in such a way as to include the full influence of rotational feedback we must proceed iteratively [*Peltier*, 1998]. We first neglect this impact and solve (2), using the complete ice and ocean loading history that this solution delivers to predict the ω_i using the methodology discussed by *Peltier* [1982] and *Wu and Peltier* [1984]. We then compute the centrifugal forcing Ψ^{R} and include the rotational forcing to construct a next order solution to (2). This process is continued until convergence is achieved.

[8] For the purpose of all of the analyses to be presented it will be assumed that the history of continental ice thickness variations is that described by the ICE-5G v1.2b model [*Peltier*, 2007a]. This model is a relatively minor variation upon the original ICE-5G model published by *Peltier* [2004]. The sole variation on the GIA model that uses this representation of glaciation history will be that associated with the viscosity model.

4. Results

[9] Figure 2 shows the predictions of the ICE-5G v1.2b models for both the non-tidal acceleration of rotation (J2-dot) datum and polar wander speed for a series of *a priori* fixed values of the viscosity assigned to the D″ layer and as a function of the viscosity in the overlying layer. The hatched regions denote the observational constraints. The red and blue dots represent the values predicted by the original ICE-5G (VM5a) model. Inspection demonstrates that without modification this model over-predicts the observed value of J2-dot and under-predicts the observed value of polar wander speed. The superimposed red and blue dashed lines on each frame represent the variations of these predictions as a function of the viscosity of the thick layer that overlies D″. When the viscosity for D″ is

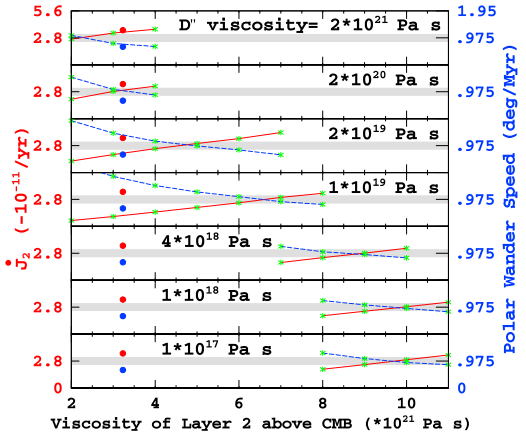

Figure 2. A large number of computational results are shown for both J2-dot and polar wander speed as a function of both the viscosity assumed to characterize the D″ layer adjacent to the core-mantle boundary and the viscosity of the overlying layer above D′ in the suite of D″ models sketched in Figure 1. The hatched region in the portion of the figure corresponding to each value of D″ viscosity indicates the observed value with appropriate error bars for both J2-dot and polar wander speed, the scales for these observables having been chosen so that the observed values for both observations and their error bars would coincide. The red and blue line in each section of the figure represent the variation of the theoretical predictions of these two observables as a function of the viscosity of the thick layer that overlies D″ for the assumed value of the viscosity in the latter region.

fixed to the value of 2×10^{21} Pa s then it will be observed that BOTH rotational anomalies are correctly predicted when the viscosity of the overlying layer is fixed to a value only slightly higher As the viscosity of D′ is reduced, inspection of the remaining frames in Figure 2 shows that the value of the viscosity in the overlying layer must increase to recover the fit to the two earth rotation anomalies. This is expected although it is not obvious that BOTH rotational anomalies will ALWAYS be capable of being fit by the same viscosity model. This strongly reinforces the notion that no other dynamical process can be contributing significantly to these anomalies. After all, as stressed by *Peltier and Luthcke* [2009], these anomalies are determined by the distinct off-diagonal and on-diagonal components of the changes in the moment of inertia tensor induced by the GIA process (see equations (4)).

[10] It remains an issue, however, as to whether there may be a way to choose among the large set of equally plausible solutions summarized in the trade-off diagram of Figure 3a. on which is plotted the allowed range of solutions for polar wander speed and J2-dot in the space of D″ viscosity and the viscosity of the overlying layer. Clearly as the D″ viscosity decreases the viscosity of the lower layer required to recover the fit increases. For D″ viscosities lower than ~5×10^{18} Pa s, however, the trade-off curve saturates as D″ is now essentially inviscid. In Figure 3b the predicted direction of true polar wander for this set of models is presented..

Taking the International Latitude Service (ILS) data to best represent the observed direction, the viscosity of D″ is bounded below by a value of approximately 10^{19} Pa s and the viscosity of the overlying layer is bounded above by a viscosity of approximately 5×10^{21} Pa s. Also shown is the Hipparcos estimate of polar wander direction [e.g., *Gross and Vondrak*, 1999] which is somewhat to the east of the direction determined by the ILS data. Since the Hipparcos estimate extends the observations of polar wander direction further into the future from 1979, at which point the ILS measurements were discontinued, these astrometrically derived inferences could be recording the onset of an influence in addition to the Late Quaternary ice-age.

[11] That some such influence must be active is made clear by Figure 4 on which are shown the predictions of the model of GIA related ice-age influence of the time dependence of the degree two and order one Stokes coefficients in the spherical harmonic expansion of the gravitational field of the planet that is being measured by the GRACE satellites. These C21-dot and S21-dot coefficients are plotted on Figure 4 in a format identical to that used for Figure 2. The values taken to represent the GRACE observed quantities are those from *Peltier and Luthcke* [2009] based upon an original inversion of the raw GRACE range-rate data in which the predictions of the original ICE-5G (VM2) v1.2b model were employed as assumed known a priori best estimates. The analysis then delivered corrections to these assumed known coefficients. The red and blue dots on each of the separate plates of Figure 4 are the predictions of the ICE-5G (VM5a) model, which has no D″ layer. The solid red and dashed blue lines are predictions for a range of overlying layer viscosities for fixed values of D″ viscosity. On each plate the vertical black lines represent the range of lower layer viscosities which, for the selected value of D″

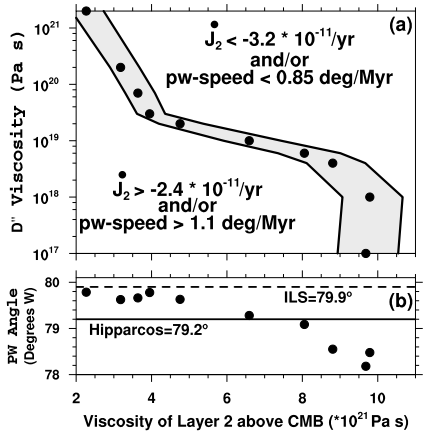

Figure 3. (a) A trade-off diagram describing the relationship between the viscosity assumed for the D″ layer and that of the lower mantle layer which overlies it that is required in order that both observables are fit by the same model of the GIA process. (b) The predicted direction of polar wander for the complete set of models which have been show to simultaneously fit both observations. The observed direction consistent with the International Latitude Service data set is compared to the direction determined astrometrically by *Gross and Vondrak* [1999].

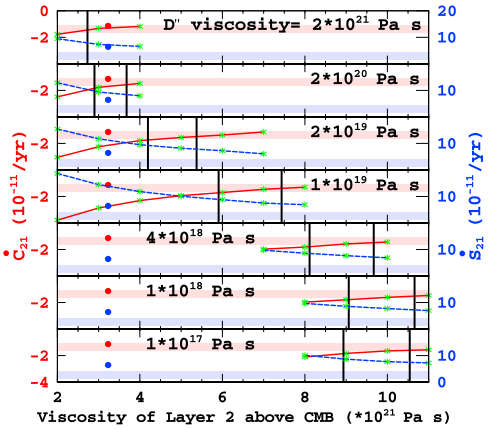

Figure 4. Predictions of the time dependent Stokes coefficients of degree 2 and order 1 for the same set of viscosity models employed to construct Figure 2. the observed values of these coefficients together with their error bars are those recently determined by *Peltier and Luthcke* [2009] and are indicated by the hatched regions on the figure. Notable is the fact that, although the GIA models are able to reasonable well reconcile the observed value of the C21-dot coefficient, S21-dot cannot be explained by the models. As discussed in the text, this is a consequence of the fact that the global model of the GIA process employed n these analyses does not include the influence upon earth's rotational state associated with the modern melting of land ice due to the global warming process.

viscosity, it is possible to fit both the polar wander speed and J2-dot observables. .Although it is always possible to fit the C21-dot value observed by GRACE, it is NEVER possible to simultaneously fit the observed S21-dot value.

5. Summary and Conclusions

[12] The inability of the model of the GIA process to fit both of the time dependent degree 2 and order 1 Stokes coefficients may be viewed as odd and suggestive of a fundamental flaw in the model. However, it must be understood that the GRACE observations pertain to an entirely distinct (and short) range of time from launch of the satellite system in 2002 until the present. In this most recent interval of time the onset of intense melting of land ice near the poles has begun and is clearly observed by GRACE itself [e.g., *Velicogna and Wahr*, 2006a, 2006b; *Peltier*, 2009] and this constitutes a strong forcing upon Earth's rotational state in addition to that associated with Late Quaternary ice-age influence . Indeed it has recently been established that both polar wander speed and the non-tidal acceleration of rotation began to perceptibly deviate from the rates explained by Late Quaternary ice-age influence in the mid- 1990's just prior to the launch of GRACE [*Gross and Poutanen*, 2009]. This is an expected impact of global warming. The deviation of the GRACE observed from the ice-age related predictions of the time dependent degree 2 and order 1 Stokes coefficients will provide additional constraints upon *a priori* models of the modern rates and locations of significant land ice melting.

References

Clark, J. A., W. E. Farrell, and W. R. Peltier (1978), Global changes in postglacial sea level: A numerical calculation, *Quat. Res.*, *9*, 265–287, doi:10.1016/0033-5894(78)90033-9.

Dahlen, F. A. (1976), The passive influence of the oceans upon the rotation of the Earth, *Geophys. J. R. Astron. Soc.*, *46*, 363–406.

Dziewonski, A. M., and D. L. Anderson (1981), Preliminary reference Earth model, *Phys. Earth Planet. Inter.*, *25*, 297–356, doi:10.1016/0031-9201(81)90046-7.

Farrell, W. E., and J. A. Clark (1976), On postglacial sea level, *Geophys. J. R. Astron. Soc.*, *46*, 647–667.

Gross, R. S., and M. Poutanen (2009), Geodetic observations of glacial isostatic adjustment, *Eos Trans. AGU*, *90*(41), doi:10.1029/2009EO410004.

Gross, R. S., and J. Vondrak (1999), Astrometric and space-geodetic observations of polar wander, *Geophys. Res. Lett.*, *26*(14), 2085–2088, doi:10.1029/1999GL900422.

Lin, J.-F., V. V. Struzhkin, S. D. Jacobsen, M. Y. Hu, P. Chow, J. Kung, H. Liu, H. Mao, and R. J. Hemley (2005), Spin transition of iron in magnesiowustite in the Earth's lower mantle, *Nature*, *436*, 377–380, doi:10.1038/nature03825.

Murakami, M., K. Hirose, K. Kawamura, N. Sata, and Y. Ohishi (2004), Post-perovskite phase transition in $MgSiO_3$, *Science*, *304*, 855–858, doi:10.1126/science.1095932.

Peltier, W. R. (1974), The impulse response of a Maxwell Earth, *Rev. Geophys.*, *12*, 649–669, doi:10.1029/RG012i004p00649.

Peltier, W. R. (1976), Glacial isostatic adjustment II: The inverse problem, *Geophys. J. R. Astron. Soc.*, *46*, 669–706.

Peltier, W. R. (1982), Dynamics of the ice-age Earth, *Adv. Geophys.*, *24*, 1–146.

Peltier, W. R. (1994), Ice-Age paleotopography, *Science*, *265*, 195–201, doi:10.1126/science.265.5169.195.

Peltier, W. R. (1996), Mantle viscosity and ice-age ice-sheet topography, *Science*, *273*, 1359–1364, doi:10.1126/science.273.5280.1359.

Peltier, W. R. (1998), Postglacial variations in the level of the sea: implications for climate dynamics and solid-Earth geophysics, *Rev. Geophys.*, *36*, 603–689, doi:10.1029/98RG02638.

Peltier, W. R. (2004), Global glacial isostasy and the surface of the ice-age Earth: the ICE-5G(VM2) model and GRACE, *Annu. Rev. Earth Planet. Sci.*, *32*, 111–149, doi:10.1146/annurev.earth.32.082503.144359.

Peltier, W. R. (2007a), History of Earth rotation, in *Treatise on Geophysics*, vol. 9, *Evolution of the Earth*, edited by D. Stevenson, chap. 10, pp. 243–293, Elsevier, Amsterdam.

Peltier, W. R. (2007b), Mantle dynamics and the D″ layer: Impacts of the post-Perovskite phase, in *Post-Perovskite: The Last Mantle Phase Transition*, *Geophys. Monogr. Ser*, vol. 174, edited by K. Hirose et al., pp. 217–227, AGU, Washington, D. C.

Peltier, W. R. (2009), Closure of the budget of global sea level rise over the GRACE era: The importance and magnitudes of the required corrections for the influence of global glacial isostatic adjustment, *Quat. Sci. Rev.*, doi:10.1016/j.quascirev.2009.04.004.

Peltier, W. R., and J. T. Andrews (1976), Glacial isostatic adjustment I: The forward problem, *Geophys. J. R. Astron. Soc.*, *46*, 605–646.

Peltier, W. R., and R. Drummond (2008), Rheological stratification of the lithosphere: A direct inference based upon the geodetically observed pattern of the glacial isostatic adjustment of the North American continent, *Geophys. Res. Lett.*, *35*, L16314, doi:10.1029/2008GL034586.

Peltier, W. R., and S. B. Luthcke (2009), ON the origins of Earth rotation anomalies: New insights on the basis of both "paleogeodetic" data and Gravity Recovery and Climate Experiment (GRACE) data, *J. Geophys. Res.*, *114*, B11405, doi:10.1029/2009JB006352.

Peltier, W. R., W. E. Farrell, and J. A. Clark (1978), Glacial isostasy and relative sea-level: A global finite element model, *Tectonophysics*, *50*, 81–110, doi:10.1016/0040-1951(78)90129-4.

Persson, K., A. Bengtson, G. Ceder, and D. Morgan (2006), *Ab initio* study of the composition dependence of the pressure-induced spin transition in the $(Mg_{1-x},Fe_x)O$ system, *Geophys. Res. Lett.*, *33*, L16306, doi:10.1029/2006GL026621.

Velicogna, I., and J. Wahr (2006a), Acceleration of Greenland ice mass loss in Spring 2004, *Nature*, *443*, 329–331, doi:10.1038/nature05168.

Velicogna, I., and J. Wahr (2006b), Measurements of time-variable gravity show mass loss in Antarctica, *Science*, *311*, doi:10.1126/science. 1123785.

Wu, P., and W. R. Peltier (1984), Pleistocene deglaciation and the Earth's rotation: A new analysis, *Geophys. J. R. Astron. Soc.*, *76*, 202–242.

Yuen, D. A., and W. R. Peltier (1980), Mantle plumes and the thermal stability of the D″ layer, *Geophys. Res. Lett.*, *7*(9), 625–628, doi:10.1029/GL007i009p00625.

R. Drummond and W. R. Peltier, Department of Physics, University of Toronto, 60 St. George St., Toronto, ON M5S 1A7, Canada. (peltier@atmosp.physics.utoronto.ca)